On the validation study devoted to stratified atmospheric flow over an isolated hill

Sládek I.[2/], Kozel K.[1/], Jaňour Z.[2/]

1/ U12101, Faculty of Mechanical Engineering, Czech Technical University in Prague.

2/ Institute of Thermo-mechanics, Academy of Sciences, Prague.

Abstract

The paper deals with description of the validation model, flow conditions and mainly it presents some numerical results. Reference and input data for the validation study are based on work of Eidsvik [6].

The mathematical model is based on the system of RANS-equations closed by two-equation $k - \varepsilon$ turbulence model together with wall functions. The thermal stratification is modeled using transport equation for the potential temperature. The finite volume method and the explicit Runge–Kutta time integration method are utilized for the numerics.

1   Mathematical formulation

The flow itself is assumed to be a turbulent, viscous, incompressible, stationary and indifferently/stably stratified. The mathematical model is based on the RANS approach modified by the Boussinesq approximation, according to which the following decomposition is utilized, Jaňour [1]

$$p = p_0 + p', \quad \varrho = \varrho_0 + \varrho', \quad \Theta = \Theta_0 + \Theta'$$

where $_0$ denotes synoptic scale part and $'$ concerns the deviation from the synoptic part due to local conditions. Then the governing equations can be re-casted in the conservative and vector form also using the artificial compressibility approach

$$\vec{W}_t + \begin{pmatrix} u \\ u^2 + \frac{p'}{\varrho_0} \\ uv \\ uw \\ u\Theta' \end{pmatrix}_x + \begin{pmatrix} v \\ vu \\ v^2 + \frac{p'}{\varrho_0} \\ vw \\ v\Theta' \end{pmatrix}_y + \begin{pmatrix} w \\ wu \\ wv \\ w^2 + \frac{p'}{\varrho_0} \\ w\Theta' \end{pmatrix}_z = \begin{pmatrix} 0 \\ Ku_x \\ Kv_x \\ Kw_x \\ \tilde{K}\Theta'_x \end{pmatrix}_x + \begin{pmatrix} 0 \\ Ku_y \\ Kv_y \\ Kw_y \\ \tilde{K}\Theta'_y \end{pmatrix}_y + \begin{pmatrix} 0 \\ Ku_z \\ Kv_z \\ Kw_z \\ \tilde{K}\Theta'_z \end{pmatrix}_z + \vec{f}$$

(1)

where

$$\vec{W} = (p'/\beta^2, \, u, \, v, \, w, \, \Theta')^T, \quad \vec{f} = (0, \, 0, \, +g\frac{\Theta'}{\Theta_0}, \, 0)^T$$

(2)

where $\vec{W}$ stands for the vector of unknown variables and $\vec{f}$ for the buoyancy force due to the thermal stratification.

The velocity vector components read $u, \, v, \, w$, term g is the gravity acceleration, the parameters $K, \, \tilde{K}$ refer to the turbulent diffusion coefficients and β is related to the artificial sound speed.

The synoptic scale part of the potential temperature is taken as $\Theta_0 = \Theta_w + \gamma z$ where Θ_w is the wall potential temperature and γ refers to the wall-normal potential temperature gradient to be > 0 for stable thermal stratification and $= 0$ for the indifferent one.

2 Turbulence model

Closure of the system of governing equations (1) is achieved by a standard $k - \varepsilon$ turbulence model without damping functions [8], [1]. Two additional transport equations are added to the system (1), one for the turbulent kinetic energy abbreviated by k and one for the rate of dissipation of turbulent kinetic energy denoted by ε. The thermal stratification is taken into account

$$(ku)_x + (kv)_y + (kw)_z = \left(K^{(k)} k_x\right)_x + \left(K^{(k)} k_y\right)_y + \left(K^{(k)} k_z\right)_z + P + G - \varepsilon \qquad (3)$$

$$(\varepsilon u)_x + (\varepsilon v)_y + (\varepsilon w)_z = \left(K^{(\varepsilon)} \varepsilon_x\right)_x + \left(K^{(\varepsilon)} \varepsilon_y\right)_y + \left(K^{(\varepsilon)} \varepsilon_z\right)_z +$$
$$C_{\varepsilon 1}(1 + C_{\varepsilon 3} R_f)\frac{\varepsilon}{k}\left(P + G\right) - C_{\varepsilon 2}\frac{\varepsilon^2}{k}$$
$$(4)$$

where $G = \beta_\Theta\, g\, \frac{\nu_T}{\sigma_\Theta}\, \frac{\partial \Theta}{\partial z}$ abbreviates the buoyancy term, $P = \tau_{ij}\frac{\partial v_i}{\partial x_j}$ denotes the turbulent production term for the Reynolds stress written as

$$\tau_{ij} = -\frac{2}{3}\, k\, \delta_{ij} + \nu_T\left(\frac{\partial v_i}{\partial x_j} + \frac{\partial v_j}{\partial x_i}\right) \qquad (5)$$

and the terms $K^{(k)}$, $K^{(\varepsilon)}$ stand for the diffusion coefficients represented by the following expressions
$$K^{(k)} = \nu + \frac{\nu_T}{\sigma_k}, \quad K^{(\varepsilon)} = \nu + \frac{\nu_T}{\sigma_\varepsilon}, \quad \tilde{K} = \nu + \frac{\nu_T}{\sigma_\Theta}. \qquad (6)$$

Finally, the turbulent viscosity is evaluated from

$$\nu_T = C_\mu \frac{k^2}{\varepsilon}. \qquad (7)$$

The model constants are as follows

$$C_\mu = 0.09, \quad \sigma_k = 1.0, \quad \sigma_\varepsilon = 1.3, \quad C_{\varepsilon 1} = 1.44,$$
$$C_{\varepsilon 2} = 1.92, \quad C_{\varepsilon 3} = 0.7, R_f = -\frac{G}{P}. \qquad (8)$$

Note that the buoyancy term $G = 0$ in case of neutral stratification.

3 Boundary conditions

The system (1)+(3)+(4) is solved with the following boundary conditions [1], [8]

- Inlet: $u = \frac{u^*}{\kappa}\ln\left(\frac{z}{z_0}\right)$, $v = 0$, $w = 0$, $k = \frac{u^{*2}}{\sqrt{C_\mu}}\left(1 - \frac{z}{D}\right)^2$, $\varepsilon = \frac{C_\mu^{3/4} \cdot k^{3/2}}{\kappa \cdot z}$, $\Theta' = 0$
  where the expression for u velocity component is used to cover the boundary layer depth D while constant value $u = U_0$ is prescribed above the boundary layer depth up to the top of computational domain.

- Outlet: homogeneous Neumann conditions for all quantities

- Top: $u = U_0$, $v = 0$, $\frac{\partial w}{\partial z} = 0$, $\frac{\partial k}{\partial z} = 0$, $\frac{\partial \varepsilon}{\partial z} = 0$, $\frac{\partial C}{\partial z} = 0$, $\frac{\partial \Theta'}{\partial z} = 0$

- Wall: standard wall functions are applied and $\frac{\partial C}{\partial n} = 0$ for the concentration and $\Theta' = 0$ for the potential temperature deviation which is equivalent to $\Theta_0 = 300\,K$

where U_0 represents the free-stream velocity magnitude, u^* is the friction velocity, $\kappa = 0.40$ denotes the von Karman constant, z_0 represents the roughness parameter and the parameter D refers to the boundary layer depth.

The wall–function approach enable to apply a wall–coarser grid where near–wall profiles of computed quantities are reconstructed using the algebraic relations. Hence, the CPU–time of computer simulations can be reduced. Remark, that correct use of this approach is for non–separated turbulent boundary layer flows only where the production of turbulent kinetic energy is balanced by its dissipation [4]. However, the wall–functions of different forms are widely used in engineering practice for complex flow applications.

4   Validation case

A "Witch of Agnesi" symmetric 2D-hill $h(y) \equiv H/(1 + (x/1667)^2)$ of height $H = 1\,km$ and base length about $12\,km$ was selected, Eidsvik [6]. Totally three different stratified cases plus one indifferent case have been tested and compared.

Our computational domain is $< -15, +25 > \times < 0,\,10 >$ measured in km and the hill summit is located just at the stream-wise position $x = 0\,km$. The domain is divided into a structured hexahedral, non-orthogonal control cells 100x40 (40/60 cells before/after hill summit) forming the computational grid with non-uniform distribution around hill top and also close to wall using the expansion ratio parameters $ax = 1.04$ and $ay = 1.10$ leading to minimum space increments $\Delta x_{min} = 165\,m$ and $\Delta y_{min} = 20\,m$, see figures 1, 2.

The Reynolds number is $Re = 6.7 \cdot 10^8$ based on the free-stream air velocity $U_0 = 10.05\,m/s$ and the hill height H. The inlet velocity profile is "frozen" from ground height about $100\,m$ to amplify the effect of the lee-waves behind the hill under thermal stratification conditions.

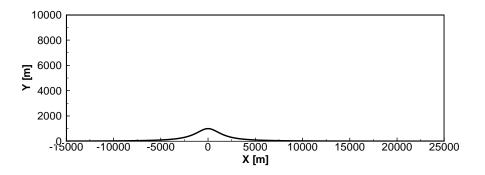Note, that details regarding grid spacing used by Eidsvick are not available in the reference paper [6].

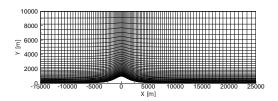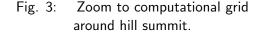Fig. 1:   Whole 2D-computational domain.

Fig. 2: Computational grid 100×40 cells.

Fig. 3: Zoom to computational grid around hill summit.

The flow–field input data as used in [6]: the free-stream air velocity $U_0 = 10.5\,m/s$, boundary layer depth of $D = 100\,m$, the friction velocity $u^* = 0.406\,m/s$, the roughness parameters $z_0 = 5\,mm$ and the Reynolds number based on U_0, hill height H and the air kinematic viscosity $\nu = 1.5 \cdot 10^{-5}\,m^2/s$ is $Re = 6.7 \cdot 10^8$.

The inlet profiles for velocity vector components u, v, w, turbulence quantities k, ε as well as for potential temperature deviation Θ' were constructed as described in the section 3.

Totally three different computations have been performed, labeling them as N0, N1, N2 and N3 as done by in [6]. Specifically, the following thermal stratifications of atmospheric boundary layer were tested

- N0-case: neutral stratification conditions $\gamma = \frac{\partial \Theta_0}{\partial z} = 0\,K/m$

- N1-case: weak stable stratification conditions $\gamma = \frac{\partial \Theta_0}{\partial z} = 3.09 \cdot 10^{-3}\,K/m$

- N2-case: middle stable stratification conditions $\gamma = \frac{\partial \Theta_0}{\partial z} = 12.36 \cdot 10^{-3}\,K/m$

- N3-case: strong stable stratification conditions $\gamma = \frac{\partial \Theta_0}{\partial z} = 27.80 \cdot 10^{-3}\,K/m$

4.1 Some numerical results

Separation zone behind hill was found in N0-case under neutral stratification conditions having separation point at $x_1 = 0.9H$ and reattachment point at $x_2 = 3.3H$ downstream from the hill top, see figure 4. The recirculation zone in our case is smaller compared to Eidsvick [6] under the same flow conditions where his separation, reattachment points are $x_1 = 0.8H$, $x_2 = 5.3H$, respectively.
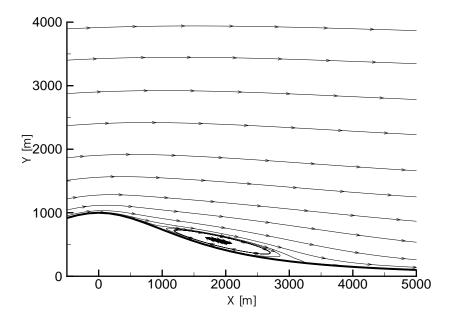
4

Fig. 4: Zoom to separation zone in N0-case under neutral stratification conditions.

Contours of the wall-normal velocity component w are shown in the following four figures 5–8 corresponding to N0-, N1-, N2- and N3-case under neutral, weak, middle and strong stratification conditions, respectively. All contours are labeled using levels of w velocity component in $[m/s]$.
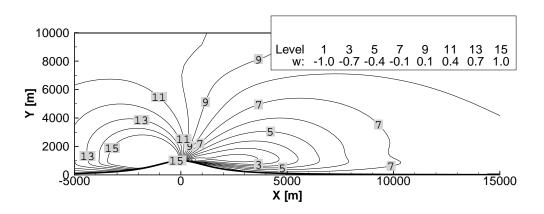

Fig. 5: Contours of the wall-normal w velocity component in N0-case under neutral stratification conditions.
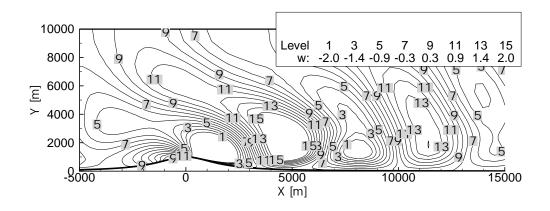
5

Fig. 6:   Contours of the wall-normal w velocity component in N1-case under weak stratification conditions.
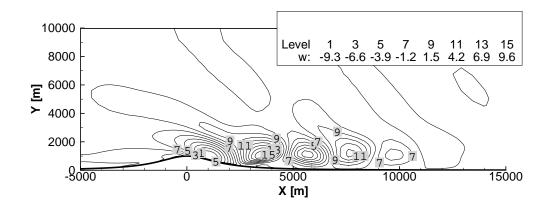

Fig. 7:   Contours of the wall-normal w velocity component in N2-case under middle stratification conditions.
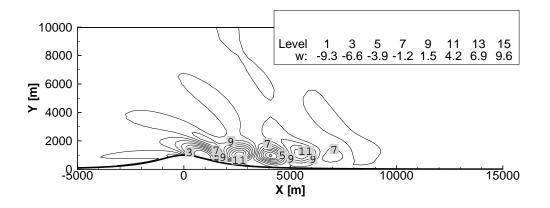

Fig. 8:   Contours of the wall-normal w velocity component in N3-case under strong stratification conditions.

The lee-waves in cases N1, N2 and N3 are very well captured as closed contours of the wall-normal w velocity component changing sign from "+" zone where the wave has an increasing slope to "-" zones where it has a decreasing slope.

6

According to theory of the internal gravitational waves [7], it is possible to estimate the wavelength of lee-waves depending on selected stratification conditions. The relation can be written as

$$\lambda = 2\pi U_0 \left(\frac{g}{\Theta_0} \frac{\partial \Theta_0}{\partial z} \right)^{-1/2} \tag{9}$$

The computed wavelength is in a reasonable agreement with the predictions by Eidsvick [6]. However, one can see the increasing difference between our predictions and theoretical wavelength values as the thermal stratification approaches the N3-case. This finding can be also attributed to a stretched nature of the computational grid which was applied mainly in the wall-normal direction along wall and it will be further investigated

- N0-case: no lee-waves present

- N1-case: $\lambda_{computed} = 6.5\,km$, $\lambda_{Eidsvick} = 6.5\,km$, $\lambda_{theoretical} = 6.3\,km$

- N2-case: $\lambda_{computed} = 4.0\,km$, $\lambda_{Eidsvick} = 3.7\,km$, $\lambda_{theoretical} = 3.1\,km$

- N3-case: $\lambda_{computed} = 2.8\,km$, $\lambda_{Eidsvick} = 2.5\,km$, $\lambda_{theoretical} = 2.1\,km$.

It is also possible to observe a decreasing tendency of the lee-waves amplitude as moving further downstream from the hill summit due to a viscous nature of flow. Note also, that a significantly increasing flow velocity magnitude was found on the lee-side of the hill as the thermal stratification was increasing.

5   Conclusion

The mathematical and numerical 3D-model suitable for thermally stratified atmospheric flow modelling has been formulated. The 2D validation test case was defined and some numerical results presented based on reference data by Eidsvik [6]. A reasonable agreement was found in wavelength of lee-waves between our predictions and those by Eidsvik.

References

[1] Jaňour Z. (2006): On the mathematical modelling of stratified atmosphere, Institute of Thermodynamics, Report T-470/06, Prague. (in Czech)

[2] Sládek I., Bodnár T., Kozel K. (2007): On a numerical study of atmospheric 2D- and 3D-flows over a complex topography with forest including pollution dispersion, Journal of Wind Engineering and Industrial Aerodynamics, Vol. 95, Issues 9–11, p. 1422-1444.

[3] Sládek, I. (2005) Mathematical modelling and numerical solution of some 2D– and 3D–cases of atmospheric boundary layer flow, PhD thesis, Czech Technical University, Prague.

[4] Wilcox D.C. (1993): Turbulence modeling for CFD, DCW Industries, Inc.

[5] Sládek I., Kozel K., Jaňour Z. (2008): On the 2D-validation study of the atmospheric boundary layer flow model including pollution dispersion, Engineering Mechanics, Vol.16, No.5, p. 323-333, 2009.

[6] Eidsvik K.J., Utnes T.: Flow separation and hydraulic transitions over hills modelled by the Reynolds equations, Journal of wind engineering and industrial aerodynamics, Vol. 67 & 68, p.403–413, 1997

[7] Holton James: An introduction to dynamic meteorology, Academic Press INC., ISBN 0-12-354360-6, 1979.

[8] Castro I.P., Apsley P.P. (1996): Flow and dispersion over topography: A comparison between numerical and laboratory data for two-dimensional flows, Atmospheric Environment, Vol.31, No.6, p.839–850.